ISSN 1054-660X, Laser Physics, 2012, Vol. 22, No. 2, pp. 441–446.

Actively Q-Switched Mode-Locked Yb-Doped Fiber Laser with High Mode-Locking Contrast[1]

T.-H. Yen[a], J.-H. Lin[b, *], and Y. Lai[a]

[a] *Department of photonics and Institute of Electro-Optical Engineering, National Chia-Tung University, Hsinchu, 300, Taiwan, China*

[b] *Department of Electro-Optical Engineering and Institute of Electro-Optical Engineering, National Taipei University of Technology, Taipei, 10608, Taiwan, China*

*e-mail: jhlin@ntut.edu.tw

Received August 19, 2011; in final form, September 9, 2011; published online December 28, 2011

Abstract—Reliable Q-switched and mode-locked operation of Yb-doped fiber lasers is investigated by employing an acousto-optic modulator (AOM) in a linear cavity configuration. The widths and shapes of the Q-switched envelopes mainly depend on the external modulation frequency of the AOM and near symmetric Q-switched pulses can be generated. Within the Q-switched envelopes, harmonic mode-locked pulses with near 100% modulation depth at the 40 MHz repetition rate are experimentally observed.

DOI: 10.1134/S1054660X12020247

1. INTRODUCTION

For generation of ultrashort pulses at near infrared wavelengths, fiber lasers provide an attractive alternative to solid-state lasers because of their reliability and compact design. In particular, ytterbium-doped fiber lasers (YDFLs) and erbium-doped fiber lasers (EDFLs) have attracted a lot of attention because of their beneficial properties for laser applications around the 1.00 and 1.55 μm wavelength range [1]. Besides, bismuth oxide erbium-doped fiber (Bi–EDFs) and bismuth-doped silica fiber have also been investigated for ultrashort short pulses and supercontinuum generation [2–5]. Various actively and passively mode-locked methods including the semiconductor optical amplifier (SOA) [6], nonlinear polarization evolution (NPE), figure eight laser scheme [7, 8], semiconductor saturable absorber mirror [9] and saturable absorbers such as graphene [10] and carbon nanotubes [11] are experimentally demonstrated. To take the advantage of the relatively wide gain bandwidth of Yb-ions, ultrashort pulse generation in YDFLs by NPE method has revealed the wide wavelength tunability [12] and can produce about 50 and 28 fs short pulsewidth with proper dispersion compensation [13, 14].

In addition to the ultrashort pulse generation, low repetition rate and high energy pulses generation in passive mode-locked (ML) YDFL and EDFL is investigated widely that can be operated in all normal dispersion or net normal dispersion region [15–23]. Besides, Q-switching operation is another focus in YDFLs since the relatively long upper-state life-time of Yb-ions can help the storage of energy from efficient diode pumping sources [24, 25]. For generating high energy pulses, Yb-doped double cladding fiber lasers (DCFLs) are usually used in accompanying with the active and passive modulator [26–29]. By using saturable absorbers such as Cr^{4+}:YAG, passively Q-switching operation with nanosecond pulse generation has been demonstrated in Yb-doped DCFL [26, 27]. Some studies on YDFLs have also been made with an active device like an acousto-optic modulator (AOM) to generate Q-switched pulses [28, 29]. The main advantage of active Q-switching is the easy control of the pulse repetition rate and the pulsewidth, whereas the disadvantage is the requirement of an additional external modulation signal.

Besides, simultaneously Q-switching and mode-locking was attained in the Yb-doped DCFL as the window time of AOM was increased. However, the time period of mode-locked pulses was not regular [29]. In comparing to Q-switched mode-locked (QML) lasers with different gain media, QML YDFLs seem to be a little lagged in research development. For example, by carefully adjusting the rear mirror position in an EDFL with an AOM, Myslinski et al. have shown that QML pulses can be generated through the mode beating and the nonlinear self-phase modulation [30, 31]. In diode pumped all solid state lasers (DPSSL), QML lasers have also been widely reported by a passive or active modulator [32–35].

In this work, with single-mode Yb-doped fiber as gain medium, we have demonstrated very stable QML operation by employing an acousto-optic modulator with a linear cavity configuration. Near symmetric Q-switched envelopes can be obtained and near 100% modulation depth of ML pulses can be observed within the envelopes. This is the first successful try to combine an AOM in diode pumped single cladding Yb-doped gain fiber for achieving stable QML opera-

[1] The article is published in the original.

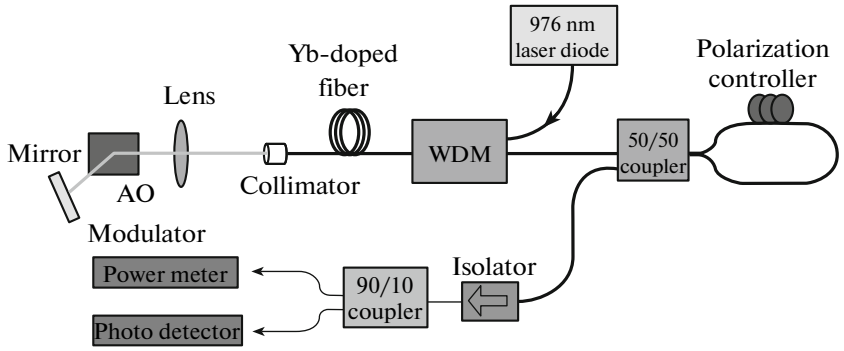

Fig. 1. Schematic diagram of the passively Q-switched mode-locked ytterbium fiber laser.

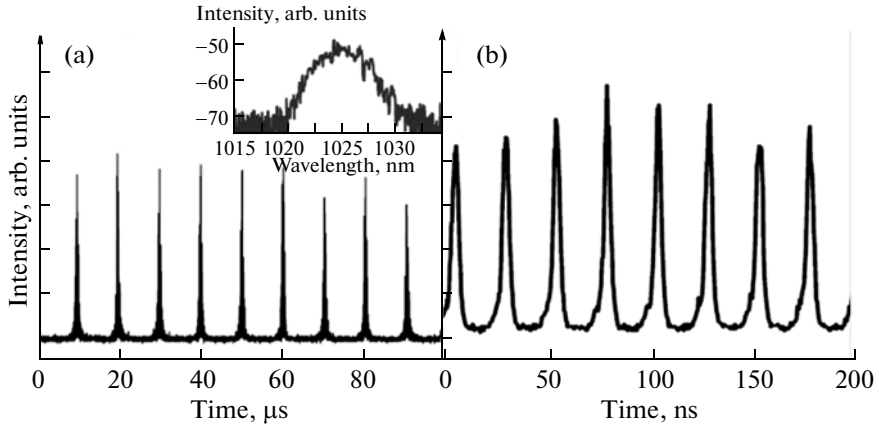

Fig. 2. (a) Time traces of Q-switched pulse trains at 100 kHz, the corresponding optical spectrum is shown in the inset. (b) Expanded time trace of a single Q-switched envelope.

tion with high mode-locking contrast in YDFLs. Besides, the satellite QML pulses were experimentally observed at lower external modulation frequency of AOM.

2. EXPERIMENTAL SETUP

The schematic setup of Q-switched pulses generation from our YDFL with a linear cavity configuration is shown in Fig. 1. A laser diode with the center wavelength of 976 nm is used to pump the Yb-doped single-mode gain fiber through a wavelength-division multiplexing (WDM) coupler. The Yb-doped fiber is 0.2 m long, with the mode-field diameter of 4.4 μm and 1200 dB/m absorption at 976 nm. The fiber loop includes a 50/50 coupler and a polarization controller with the total length of 365 cm. It acts as one of the laser end mirrors as well as the output coupler. In the other end, a collimator is used to collimate the laser lights from fiber to free space. Then, a converging lens is used to focus the laser beam onto an acousto-optic modulator (40 MHz RF, Neos Inc.) to produce the QML operation. A high reflective mirror is placed closely behind the AOM to act as the other end mirror. An isolator outside the output coupler is used to prevent the feedback of the output light into the laser cavity. Finally, we use a 90/10 coupler to divide the light into the power meter (Newport Inc.), oscilloscope (Wave Surfer 62 Xs, bandwidth 650 MHz, LeCroy Inc.) and optical spectrum analyzer (AQ 6315A, Ando Inc.) for monitoring and measurement.

3. RESULTS AND DISCUSSIONS

When the convergence lens of 7.5 cm focal length is used, simultaneously Q-switched and mode-locked operation of the laser is achieved by increasing the pump power above 80 mW. At this moment, the time period of Q-switched envelopes is not regular and the pulses have relatively large amplitude fluctuations. Stable QML output pulses with regular time period can only be seen when the pump power is above 100 mW. Figure 2a shows the time traces of stable QML pulses on the oscilloscope with the AO switching frequency around 100 kHz and the pump power of 188 mW. From the observed Q-switched envelope

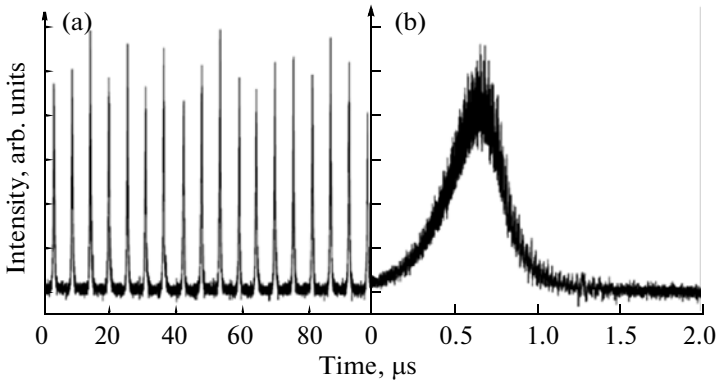

Fig. 3. (a) Time traces of Q-switched pulse trains at 180 kHz and 188 mW pump power by using the 12 cm focal lens. (b) Expanded time trace of a single Q-switched envelope.

traces in Fig. 2a, the repetition rate is almost regular and the fluctuations are relatively small. Figure 2b reveals the expanded single Q-switched envelope, where a number of discrete and periodic ML pulses with time period about 25 ns (corresponding to the repetition rate of 40 MHz) can be obviously seen. The modulation depth of ML pulses is near 100%, indicating excellent modelocking has been obtained. The corresponding optical spectrum shown in the inset of Fig. 2a indicates that the center wavelength is 1025 nm and the bandwidth is about 3.68 nm. The relatively wide lasing bandwidth indicates that some nonlinear processes such as self-phase modulation may have occurred in the laser cavity to help the mode-locking. The shape of the optical spectrum shown on the optical spectrum analyzer resembles the Gaussian function, which is also a supported indication of the ML operation.

The QML in YDFLs is seldom reported by the active AOM. In order to generate self-mode-locked pulses in Q-switched Yb-doped DCFL, Wang et al. try to weaken Q-switched effect by increasing the window time of the AOM at 20 kHz repetition rate [29]. However, it can only be seen at relative high pump power above 2.3 W and the visibility of the split peaks of ML pulse was poor. Besides, the QML pulses were experimentally demonstrated in ytterbium and aluminophosphate codoped fiber laser that was free space pumped by the Ti:sapphire laser at 915 nm [36]. In their laser setup, the optical modulator with 80 MHz RF was placed in front of the grating as a frequency shifter to produce 80 MHz mode-locked pulse. In our configuration, the AOM was placed closely in front of the end mirror so that the zeroth order and first order diffraction beams can be reflected by the end mirror simultaneously. The first order diffraction beam will experience a frequency shift of 40 MHz after it passes through the AOM. The diffraction angle of AOM is about 7.5 mrad and is much smaller than the divergence angle of the light beam, which is about 0.2 rad. After being reflected by the end mirror, parts of the first order beam will be mixed with the zeroth order beam and vice versa. After re-entering the fiber, the interference of the contributions from the first order and the zeroth order beams will result in an amplitude modulation of 40 MHz to produce the ML pulses near 100% modulation depth. Since the cavity repetition frequency is only one-third of RF of AOM about 40 MHz, we recognize that our YDFL is harmonic mode-locking by the AOM.

In order to demonstrate that the AOM played the dominant role for the mode-locking operation in our laser, we changed the focal length of the convergence lens to adjust the focus beam size on the AOM. When the lens with the focal length 12 cm was used, a larger focus spot size on the AOM was produced compared to the original case of 7.5 cm focal length. The end mirror was 16 cm away from the converging lens, and the AOM was placed in front of the mirror as close as possible. At the pump power of 188 mW and modulation frequency around 180 kHz, instead of the QML operation, only Q-switched pulses can be produced as shown in Fig. 3a. The expanded single Q-switched envelope is shown in Fig. 3b in which only small modulation patterns rather than ML pulses within the Q-switched envelope can be obviously seen. We believe this is due to the reduction of 40 MHz amplitude modulation caused by smaller mixing of first order and zeroth order beam when the beam divergence angle is reduced with a longer focus length.

When we decreased the external modulation frequency of the AOM at lower pump powers, satellite Q-switched envelope can be seen in our YDFL, in which the ML pulses still existed. Figures 4a–4f show the time traces of QML pulses on the oscilloscope at the pump power of 188 mW by lowering the AOM modulation frequency down to 5, 10, 20, 30, 40, and 60 kHz, respectively. As shown in these figures, the number of satellite pulses will increase by lowering the AOM modulation frequency. In Fig. 4a, there are about fourteen satellite pulses behind the main pulse at the 5 kHz modulation frequency. The number of satel-

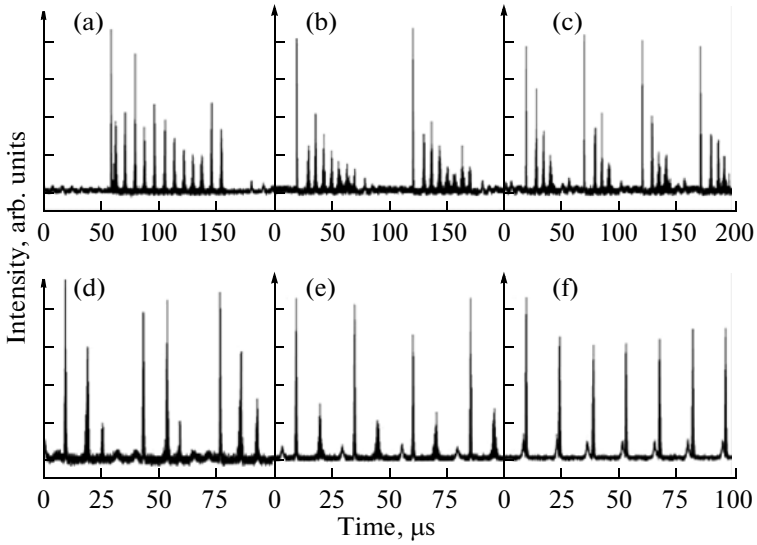

Fig. 4. Time traces of QML pulse trains at (a) 5, (b) 10, (c) 20, (d) 30, (e) 40, and (f) 60 kHz.

lite pulses will decrease to be about 9, 5, 3, 2, 1 at 10, 20, 30, 40, 60 kHz as shown in Figs. 4b–4f. The mechanism of satellite-pulses generation can be explained as shown in Fig. 5. When the main Q-switched pulse is generated after the AOM turns on, the population inversion is consumed quickly so that the gain is reduced below the loss inside the cavity. At this moment, if pump power is high-enough and continuously injected into the gain medium, it will cause the gain to exceed the loss again to result in the secondary pulse. When the AO modulation frequency becomes lower, the accumulated population of the gain medium is relative high and the window for the ON time of the AOM is longer. Therefore, the laser will have more opportunity to generate the satellite pulses and the number of generated satellite pulses will also increase accordingly.

At the pump power of 188 mW, the expanded Q-switching envelopes with the modulation frequencies at 20, 60, and 100 kHz of AOM are shown in Figs. 6a–6c. The amplitude of Q-switched envelope decreases but the width increases as the modulation frequency increases. In order to obtain the rising time τ_1, and the falling time τ_2 of the Q-switched envelopes, we fit the envelopes with the following formula [33]

$$I = \frac{I_0}{\left[e^{\frac{1.76t}{\tau_1}} + e^{-\frac{1.76t}{\tau_2}}\right]}, \quad (1)$$

where I_0 is the scaling factor. We define the pulsewidth τ and the asymmetry factor F of these Q-switched envelopes by using the relations of $\tau = (\tau_1 + \tau_2)/2$ and $F = \tau_1/\tau_2$. By the fitted solid curve, the rising time $\tau_1 =$ 0.447 μs and the falling time $\tau_2 = 0.302$ μs obtained at the 20 kHz modulation frequency are shown in Fig. 6a. The width τ is estimated to be about 0.375 μs and the asymmetry factor F is estimate to be about 1.5, which indicates a relatively large asymmetric shape. As the modulation frequency increases to 60 kHz, the rising τ_1 and the falling time τ_2 increase simultaneously as shown in Fig. 6b, so that the total width τ is increased to be 0.496 μs. If we further increase the modulation frequency to be about 100 kHz, the width τ is increased to be about 0.699 μs (Fig. 6c). In addition, the asymmetry factor F reduces to about 1, indicating that the Q-switched envelope now has a near symmetric shape. Using Eq. (1), the widths of the Q-switched envelope (squares) from 5 to 110 kHz were obtained and shown in Fig. 7. Besides, the estimated peak voltage of Q-switched envelope (triangles), in considering maximum voltage from the oscilloscope, repetition rates and the width of Q-switched envelope, for different AOM frequencies at the pump power of 188 mW are also shown in Fig. 7. The widths of Q-switched envelopes show the increasing tendency whereas the

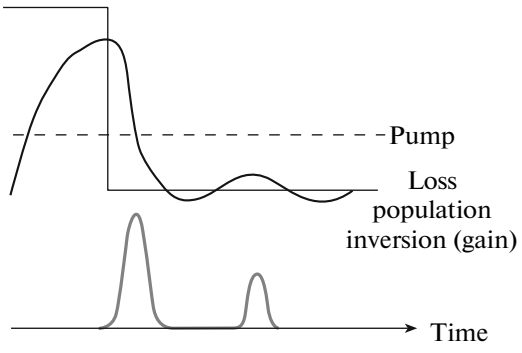

Fig. 5. Formation of satellite pulses at low modulation frequencies.

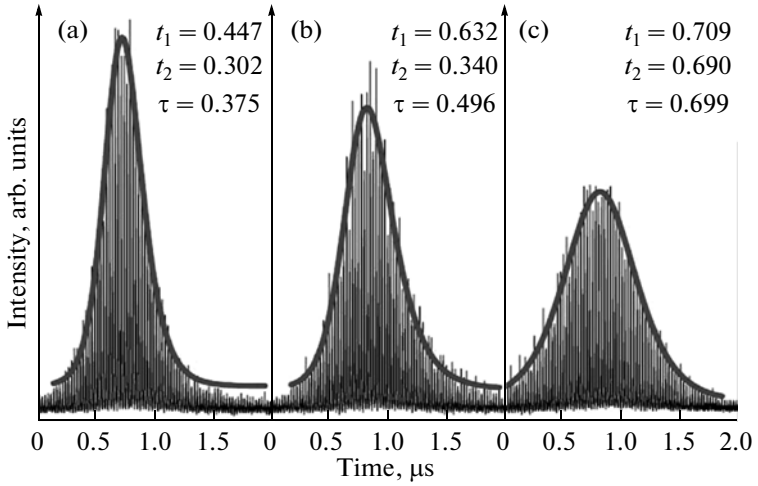

Fig. 6. Expanded temporal shape of a single QML envelope with 188 mW pumping at (a) 20, (b) 60, and (c) 100 kHz.

peak voltage of Q-switched envelope decreases as the modulation frequency increases.

4. CONCLUSIONS

Actively Q-switched mode-locked operation of an Yb-doped fiber laser has been demonstrated by simply using the single-mode Yb-doped gain fiber and an acousto-optic modulator that can be operated at a range of modulation frequencies. Within the Q-switched envelopes, mode-locked pulses with a regular 40 MHz repetition rate and near 100% modulation depth can be observed. We have confirmed that the AOM plays the dominated role simultaneously for the Q-switched and mode-locked operation of the laser. In addition, the stability, shape and pulsewidth of the generated QML envelopes will mainly depend on the pump power and the modulation frequency of the AOM. Satellite pulses will be generated at low modulation frequencies. However, near symmetric single-pulse operation can be achieved by suitably adjusting the AOM modulation frequency. To the best of our knowledge, this is the first report that successfully combines the single cladding Yb-fiber laser and an AOM for achieving stable Q-switched mode-locked operation with high modelocking contrast in Yb-doped fiber lasers.

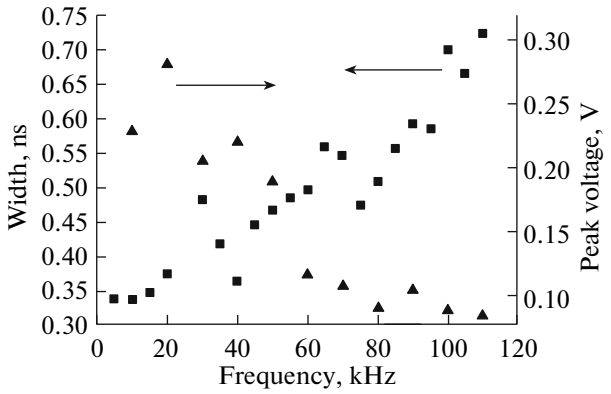

Fig. 7. Measured width and peak voltage of Q-switched envelopes versus different AOM frequencies at the pump power of 188 mW.

ACKNOWLEDGMENTS

This work is financially sponsored by National Science Council in Taiwan, R.O.C., under the grand no. NSC 99-2112-M-027-001-MY3 and NSC 99-2221-E-009-045MY3.

REFERENCES

1. A. S. Kurkov, Laser Phys. Lett. **4**, 93 (2007).
2. S. W. Harun, R. Akbari, H. Arof, and H. Ahmad, Laser Phys. Lett. **8**, 449 (2011).
3. M. R. A. Moghaddam, S. W. Harun, R. Akbari, and H. Ahmad, Laser Phys. **21**, 913 (2011).
4. M. R. A. Moghaddam, S. W. Harun, R. Akbari, and H. Ahmad, Laser Phys. Lett. **8**, 369 (2011).
5. A. P. Luo, Z. C. Luo, W. C. Xu, V. V. Dvoyrin, V. M. Mashinsky, and E. M. Dianov, Laser Phys. Lett. **8**, 601 (2011).
6. H. Feng, W. Zhao, S. Yan, and X. P. Xie, Laser Phys. **21**, 404 (2011).
7. X. H. Li, Y. S. Wang, W. Zhao, W. Zhang, Z. Yang, X. H. Hu, H. S. Wang, X. L. Wang, Y. N. Zhang, Y. K. Gong, C. Li, and D. Y. Shen, Laser Phys. **21**, 940 (2011).
8. J. C. Hernandez-Garcia, O. Pottiez, R. Grajales-Coutino, B. Ibarra-Escamilla, E. A. Kuzin, J. M. Estudillo-Ayala, and J. Gutierrez-Gutierrez, Laser Phys. **21**, 1518 (2011).
9. Y. J. Song, M. L. Hu, C. L. Gu, L. Chai, C. Y. Wang, and A. M. Zheltikov, Laser Phys. Lett. **7**, 230 (2010).

10. H. Zhang, D. Y. Tang, L. M. Zhao, Q. L. Bao, K. P. Loh, B. Lin, and S. C. Tjin, Laser Phys. Lett. **7**, 591 (2010).
11. J. C. Travers, J. Morgenweg, E. D. Obraztsova, A. I. Chernov, E. J. R. Kelleher, and S. V. Popov, Laser Phys. Lett. **8**, 144 (2011).
12. L. J. Kong, X. S. Xiao, and C. X. Yang, Laser Phys. Lett. **7**, 834 (2010).
13. F. O. Ilday, J. R. Buckley, H. Lim, F. W. Wise, and W. G. Clark, Opt. Lett. **28**, 1365 (2003).
14. X. Zhou, D. Yoshitomi, Y. Kobayashi, and K. Torizuka, Opt. Express **16**, 7055 (2008).
15. M. Zhang, L. L. Chen, C. Zhou, Y. Cai, L. Ren, and Z. G. Zhang, Laser Phys. Lett. **6**, 657 (2009).
16. X. Tian, M. Tang, P. Ping Shum, Y. Gong, C. Lin, S. Fu, and T. Zhang, Opt. Lett. **34**, 1432 (2009).
17. S. Kobtsev, S. Kukarin, and Y. Fedotov, Opt. Express **16**, 21936 (2008).
18. L. J. Kong, X. S. Xiao, and C. X. Yang, Laser Phys. Lett. **7**, 359 (2010).
19. J. H. Lin, D. Wang, and K. H. Lin, Laser Phys. Lett. **8**, 66 (2011).
20. L. R. Wang, X. M. Liu, and Y. K. Gong, Laser Phys. Lett. **7**, 63 (2010).
21. D. Mao, X. M. Liu, L. R. Wang, X. H. Hu, and H. Lu, Laser Phys. Lett. **8**, 134 (2011).
22. B. N. Nyushkov, V. I. Denisov, S. M. Kobtsev, V. S. Pivtsov, N. A. Kolyada, A. V. Ivanenko, and S. K. Turitsyn, Laser Phys. Lett. **7**, 661 (2010).
23. L. R. Wang, X. M. Liu, Y. K. Gong, D. Mao, and H. Feng, Laser Phys. Lett. **8**, 376 (2011).
24. A. V. Kiryanov and Yu. O. Barmenkov, Laser Phys. Lett. **3**, 498 (2006).
25. I. L. Villegas, C. Cuadrado-Laborde, J. Abreu-Afonso, A. Diez, J. L. Cruz, M. A. Martinez-Gamez, and M. V. Andres, Laser Phys. Lett. **8**, 227 (2011).
26. M. Laroche, H. Gilles, S. Girard, N. Passilly, and K. Alt-Ameur, IEEE Photon. Technol. Lett. **18**, 764 (2006).
27. L. Pan, I. Utkin, and R. Fedosejevs, IEEE Phton. Technol. Lett. **19**, 1979 (2007).
28. C. C. Renaud, R. J. Selvas-Aguilar, J. Nilsson, P. W. Turner, and A. B. Grudinin, IEEE Phton. Technol. Lett. **11**, 976 (1999).
29. Y. Wang, A. Martinez-Riosc, and H. Poa, Opt. Commun. **224**, 113 (2003).
30. P. Myslinski, J. Chrostowski, J. A. Koningstein, and Jay R. Simpson, IEEE J. Quantum Electron. **28**, 371 (1992).
31. P. Myslinski, J. Chrostowski, J. A. Koningstein, and J. R. Simpson, Appl. Opt. **32**, 286 (1993).
32. J. H. Lin, K. H. Lin, H. H. Hsu, and W. F. Hsieh, Laser Phys. Lett. **5**, 276 (2008).
33. J. H. Lin, H. R. Chen, H. H. Hsu, M. D. Wei, K. H. Lin, and W. F. Hsieh, Opt. Express **16**, 16538 (2008).
34. J. K. Jabczyski, W. Zendzian, and J. Kwiatkowski, Opt. Express **14**, 2184 (2006).
35. J. H. Lin, C. C. Huang, and K. H. Lin. Laser Phys. **20**, 1881 (2010).
36. J. Porta, A. B. Grudinin, Z. J. Chen, J. D. Minelly, and N. J. Traynor, Opt. Lett. **23**, 615 (1998).